ORGANIC PROCESS RESEARCH & DEVELOPMENT
OPR&D

pubs.acs.org/OPRD

Communication

# Nontraditional Application of the Photo-Fenton Process: A Novel Strategy for Molecular Construction Using Formamide and Flow Chemistry

Marialy N. Sanabria, Milene M. Hornink, Valquíria G. Correia, and Leandro H. Andrade*

Cite This: https://dx.doi.org/10.1021/acs.oprd.0c00057

Read Online

ACCESS | Metrics & More | Article Recommendations | Supporting Information

**ABSTRACT:** Instead of destroying organic compounds, for the first time the photo-Fenton reaction was employed to construct them. Oxindole and spiro-oxindole scaffolds, which are frequently found in natural products, were selected as molecular targets. The development of a photochemical flow reactor employing the photo-Fenton reaction in formamide resulted in an excellent synthetic methodology for oxindoles. Non-anhydrous conditions are required, and readily available chemicals and mild conditions are employed. Also, novel synthetic approaches for new spiro compounds were efficiently developed using functionalized oxindoles as key intermediates.

**KEYWORDS:** *photo-Fenton, formamide, construction, oxindoles, spiro-oxindoles*



## 1. INTRODUCTION

The Fenton reaction was discovered nearly 125 years ago when H. J. H. Fenton found that iron in combination with hydrogen peroxide can oxidize tartaric acid.[1] Since then, the chemical nature of this process has been explored. In the main reaction, $Fe^{2+}$ reacts with $H_2O_2$ in an acidic medium to generate hydroxyl radical, which is a nonselective and powerful oxidant that is traditionally used for the mineralization of organic compounds.[2]

Over the years, several studies of the Fenton reaction have revealed some process disadvantages, such as a narrow pH range and accumulation of $Fe^{3+}$ in the reaction medium as a consequence of the inefficient regeneration of $Fe^{2+}$.[2] In order to improve the traditional Fenton process, heterogeneous Fenton,[3] electro-Fenton,[4] and photo-Fenton[5] processes have emerged.

The photo-Fenton process is currently considered an advanced oxidation process (AOP) that is widely applied for the treatment of industrial wastewaters. This photochemical methodology employs UV light to increase the rate of reduction of $Fe^{3+}$ to $Fe^{2+}$.[5] Consequently, fast generation of hydroxyl radical and the application of small amount of catalyst ($Fe^{2+}$) can be achieved.

Inspired by all of these features, we found the opportunity to create a novel and nontraditional application of the photo-Fenton process to synthesize organic compounds using formamide and flow chemistry as key components (Figure 1).

For our purpose, oxindoles[6−9] and spiro-oxindoles[10−13] were chosen as molecular targets, since these scaffolds are widespread in natural products with important biological activities (Figure 2). Therefore, the development of general and fast synthetic methodologies to access oxindoles and spiro-oxindoles with structural diversity is highly desirable.

Considering the degradation profile of the photo-Fenton process, a continuous flow methodology was designed that avoids overexposure of organic compounds to UV light and Fenton's reagents (Scheme 1). Our strategy relies on the fast reaction of the hydroxyl radical with formamide (**2**) to generate another radical, carbamoyl, which can react with acceptors (acrylamides **1**).[14] After tandem addition−cyclization−rearomatization steps, the desired heterocycles (oxindoles **3**) are produced. In addition, functionalized oxindoles can be applied as key intermediates for novel spiro compounds (**4**−**6**).

## 2. RESULTS AND DISCUSSION

Our initial experiments were dedicated to the evaluation of the light source for the photo-Fenton process in the presence of formamide and the radical acceptor *N*-methyl-*N*-phenylmethacrylamide (**1a**). Phosphor light, a blue light-emitting diode, and UV light (450 W Hg lamp) were selected to perform the reactions under batch conditions (Table S1). A glass flask containing formamide, chemicals for hydroxyl radical generation (Fenton's reagents: hydrogen peroxide, sulfuric acid, and $FeSO_4$), and **1a** was exposed to each light source for 30 min. Only the reaction exposed to UV light (450 W Hg lamp) was able to produce the desired heterocycle, oxindole **3a**, after 30 min (60% conversion). The high light output and the emission spectrum of the Hg lamp were indispensable to achieve such a good result in a short light exposure time. We chose the Hg lamp to set up a flow photochemical reactor for continuous operation.

**Special Issue:** Flow Chemistry Enabling Efficient Synthesis

**Received:** February 14, 2020
**Published:** April 8, 2020

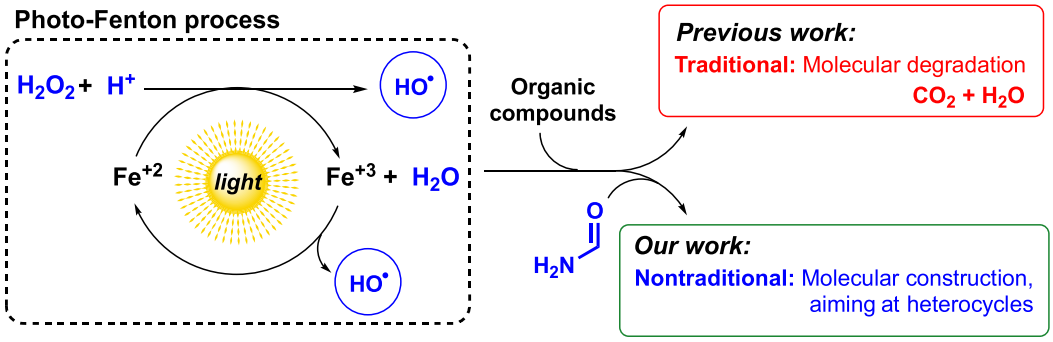


**Figure 1.** Traditional and nontraditional applications of the photo-Fenton process.

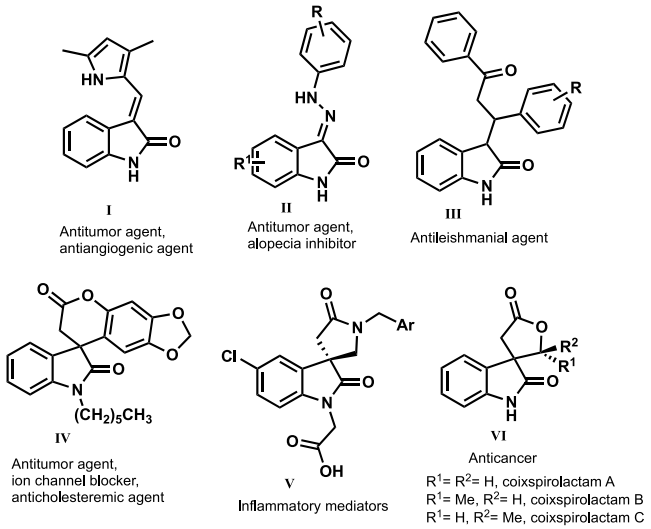


**Figure 2.** Selected examples of bioactive oxindoles and spirooxindoles.

The continuous flow photochemical reactor employed a 450 W Hg UV lamp that was inserted in a glass filter sleeve (Pyrex). Both the UV lamp and filter sleeve were inserted into a quartz immersion well. A tube reactor (volume = 1 mL) was wrapped around the quartz immersion well and connected to two syringes via a Y-adapter.

The photo-Fenton reaction of **1a** in *N*-methylformamide (**2b**) was chosen as model system to perform under continuous flow conditions. One syringe was loaded with **1a** (0.4 M), sulfuric acid (0.4 M), and $FeSO_4$ (0.004 M; 1 mol %) in *N*-methylformamide. The other syringe was loaded with $H_2O_2$ (0.8 M) in *N*-methylformamide. A syringe pump was used to infuse the two solutions through the photoreactor. The results are summarized in Table 1.

Fortunately, our initial experiments under the continuous flow conditions revealed excellent performance to produce the desired oxindole **3k**. After a residence time ($t_R$) of 10 min, the starting material was completely transformed into the desired product (Table 1, entry 1). Aiming at high productivities, we employed a high concentration of **1a** (final concentration inside the reactor = 200 mmol/L), and excellent results were observed (full conversion). Even after this excellent performance, different reaction conditions (varying the iron and hydrogen peroxide concentrations, the temperature, and the residence time) were evaluated. A smaller amount of $Fe^{2+}$ (1 mol % $FeSO_4 \cdot 7H_2O$) still provided full conversion of **3k** (Table 1, entry 2). When the oxidant ($H_2O_2$) concentration was reduced, a decrease in the reaction rate was observed (Table 1, entry 3). This result can be explained by the important role of hydrogen peroxide in the reaction mechanism, involving hydroxyl radical generation. A set of reactions at different temperatures (55, 45, 40, and 25 °C) were performed under continuous flow conditions with $t_R$ = 10 min. In all cases, we observed full conversion of the starting material to the desired product (Table 1, entries 4−7), even when formamide (**2a**) was used as the carbamoyl radical precursor (Table 1, entry 8).

**Scheme 1. Molecular Construction Using the Photo-Fenton Reaction**

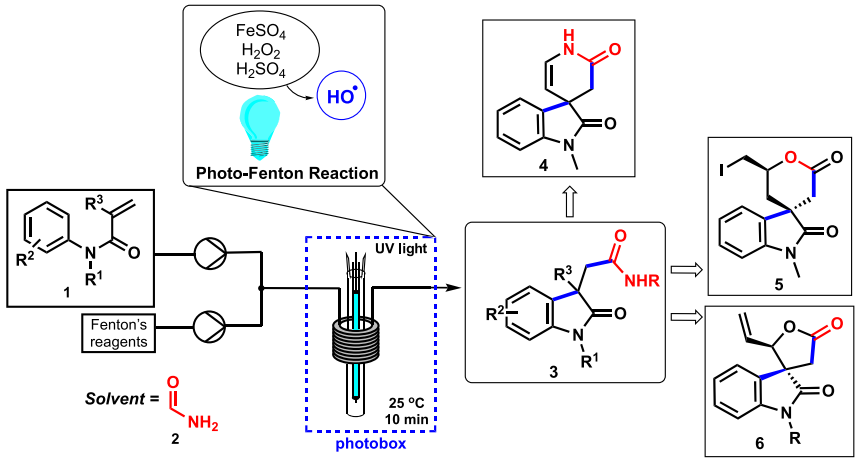




https://dx.doi.org/10.1021/acs.oprd.0c00057
Org. Process Res. Dev. XXXX, XXX, XXX−XXX

**Table 1. Synthesis of Oxindoles 3a and 3k via the Photo-Fenton Reaction in Formamide and *N*-Methylformamide, Respectively, under Continuous Flow Conditions**[a]

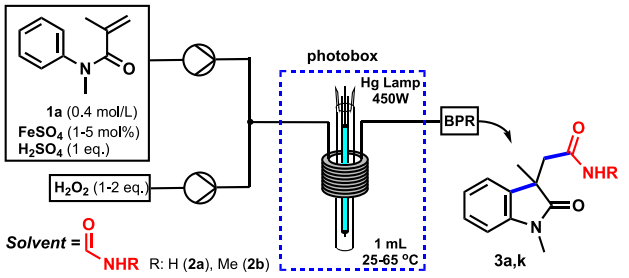


| entry | R | $FeSO_4$ (mol %) | equiv of $H_2O_2$ | $T$ (°C) | yield of **3** (%)[b] |
|---|---|---|---|---|---|
| 1 | Me | 5 | 2 | 65 | 100 |
| 2 | Me | 1 | 2 | 65 | 100 |
| 3 | Me | 1 | 1 | 65 | 72 |
| 4 | Me | 1 | 2 | 55 | 100 |
| 5 | Me | 1 | 2 | 45 | 100 |
| 6 | Me | 1 | 2 | 40 | 100 |
| 7 | Me | 1 | 2 | 25 | 100 |
| 8 | H | 1 | 2 | 25 | 100 |
| 9[c] | H | 1 | 2 | 25 | 41 |
| 10[d] | H | 1 | 2 | 25 | 11 |

[a]Reaction conditions inside the reactor: **1a** (0.2 mol/L), $H_2SO_4$ (0.2 mol/L), $FeSO_4$ (1−5 mol %), $H_2O_2$ (30% aqueous solution, 1−2 equiv), and formamide (R = H) or *N*-methylformamide (R = Me) as the solvent; residence time ($t_R$) = 10 min; reactor volume = 1 mL; 450 W Hg lamp; back-pressure regulator (BPR) set at 75 psi. [b]Conversions were determined by GC/MS analysis. [c]$t_R$ = 5 min. [d]$t_R$ = 2.5 min.

We also carried out the reaction with very short residence times (5 and 2.5 min) at room temperature. However, the starting material **1a** was not fully consumed in either case (Table 1, entries 9 and 10). Since we did not consider increasing reaction temperature, we chose $t_R$ = 10 min and room temperature for further studies.

Having established the optimal flow conditions, we turned our attention to the substrate scope (Figure 3). The reactivities of several *N*-arylacrylamides toward the photo-Fenton process in formamide or *N*-methylformamide were evaluated, and a variety of 3,3-disubstituted oxindoles **3a−n** were obtained in good to excellent yields.

The influence of the substituents on the aromatic ring of *N*-methyl-*N*-arylmethacrylamides **1** was evaluated. Several functional groups were tolerated, including *p*-Me, *p*-OMe, *p*-Cl, *o*-Ph, and *m*-OMe substituents. Among the para substituents, both electron-donating and electron-withdrawing groups gave oxindoles **3b−d** in good yields. When the *o*-phenyl-substituted *N*-methyl-*N*-arylacrylamide was evaluated, oxindole **3e** was obtained in good yield. The *m*-methoxy-substituted *N*-methyl-*N*-arylmethacrylamide provided a mixture of regioisomers **3j** as expected (81% yield; 2:3 ratio of isomers). *N*-Methyl-*N*-phenylacrylamides containing a benzyl or allyl group provided oxindoles **3f** and **3g** in high yields. *N*-Arylacrylamides containing different N-protecting groups such as benzyl and Boc were evaluated. However, only the *N*-Bn-protected acrylamides were compatible with this transformation, providing oxindoles **3h** and **3i** in excellent yields. In the case of *N*-arylacrylamides containing *N*-Boc and free N−H, no reaction was observed, and the starting material was recovered. Finally, the carbamoyl radical generated from *N*-methylformamide was used to produce oxindoles **3k−n** in good yields.

Next, the reaction mechanism was investigated. Some control experiments were performed under continuous flow conditions at room temperature (Figure 4A). One experiment without illumination gave only traces of the desired product **3a**. This result reveals the main role of the UV light, namely, the photoreduction of $Fe^{3+}$ to $Fe^{2+}$, which is also known in the traditional photo-Fenton process.[5] Another experiment was carried out to evaluate the possibility of generating hydroxyl radical from direct photolysis of $H_2O_2$ without iron ($FeSO_4$). In this case, only the starting material was observed.

On the basis of these results, a plausible mechanism for this reaction is presented in Figure 4B. First, the photo-Fenton reaction is responsible for hydroxyl radical generation as follows: hydrogen peroxide reacts with $Fe^{2+}$ to produce hydroxyl radical, $Fe^{3+}$, and water, and then $Fe^{3+}$ is reduced to $Fe^{2+}$ mediated by UV light.[5] Once formed, hydroxyl radical removes a hydrogen from the formamide, generating the desired carbamoyl radical. In the presence of $\alpha,\beta$-unsaturated amides (*N*-arylacrylamides **1a−n**), the carbamoyl radical can add to the C−C double bond to give radical **I**, followed by intramolecular cyclization. Finally, hydroxyl radical or carbamoyl radical can remove a hydrogen from cyclic radical **II** to regenerate the aromatic ring.

Aiming to apply the oxindoles for the synthesis of novel spiro compounds, we designed key intermediates **3g** and **3h** containing an allyl group properly attached to carbon C-3 (Scheme 2). Fortunately, these oxindoles were efficiently synthesized using the photo-Fenton reaction in formamide, and the desirable allyl group remained intact.

Initially, a spiro[oxindole-3,4-dihydropyridin-2-one] core was efficiently created after oxidative cleavage of the C=C bond and thermal cyclization (Scheme 2A). The protocol involved ruthenium-catalyzed oxidative cleavage to afford aldehyde *int*-**4**.[15] Upon heating of the crude material, thermal cyclization gave the desired product, spiro-[oxindole-3,4-dihydropyridin-2-one] **4**, in 83% overall yield.

The second spiro scaffold was spiro[oxindole-$\delta$-lactone] **5**. An iodolactonization protocol was applied to oxindole **3g**, and the spiro compound **5** was obtained as a single diastereomer (Scheme 2B). The reaction was performed with $I_2$ and water for 1.5 h at 0 °C.[16] The first step is iodonium ion formation at the allyl group, followed by attack of the amide carbonyl group from the opposite side of the iodonium ion to give an iminium ion intermediate. Hydrolysis of this iminium can afford **5**. (A mechanism proposal and NMR analysis are described in the Supporting Information).

Finally, a spiro[oxindole-$\gamma$-lactone] scaffold was created using a one-pot protocol (Scheme 2C). The first step was an allylic hydroxylation reaction mediated by selenium dioxide.[17] Since the selenium coproduct is selenous acid, in situ lactonization gave the desired spiro[oxindole-$\gamma$-lactones] **6a** and **6b**. This reaction was diastereoselective for both oxindoles (**6a** and **6b**; 2:1 dr). (For NMR analysis, see the discussion in the Supporting Information).

It is noteworthy that these synthetic routes represent novel accesses to three different spiro compounds, spiro[oxindole-3,4-dihydropyridin-2-one], spiro[oxindole-$\delta$-lactone], and spiro[oxindole-$\gamma$-lactone].


https://dx.doi.org/10.1021/acs.oprd.0c00057
Org. Process Res. Dev. XXXX, XXX, XXX−XXX

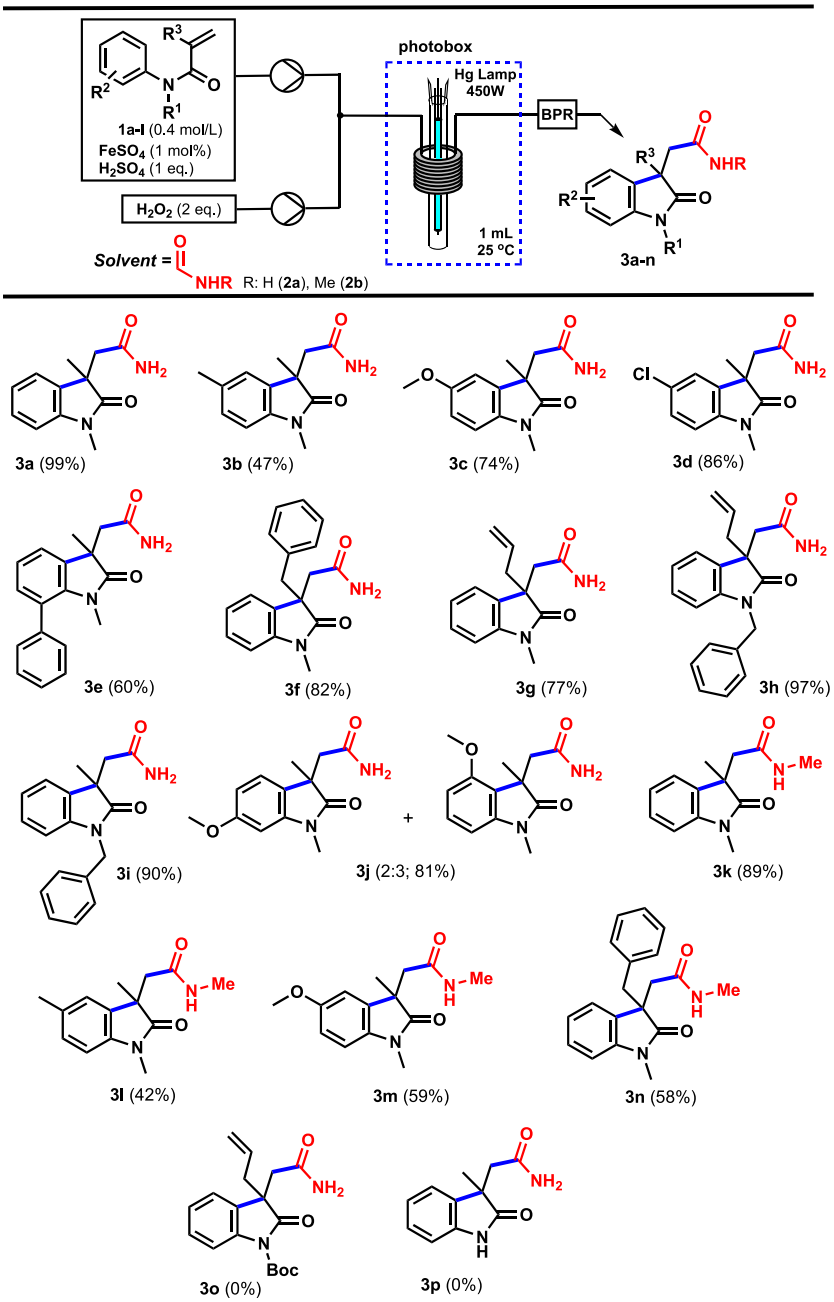


**Figure 3.** Continuous flow production of oxindoles **3a**–**n** using the photo-Fenton reaction in formamide or *N*-methylformamide. Isolated yields are reported.

## 3. CONCLUSION

For the first time, the photo-Fenton process in formamide was employed to construct heterocycles under continuous flow conditions. The fast generation of hydroxyl and carbamoyl radicals by the photo-Fenton reaction allowed the development of an excellent synthetic methodology for oxindoles. Our synthetic strategy represents a step-forward protocol since non-anhydrous conditions are required and readily available chemicals and mild conditions are employed. In addition, allyl oxindoles were designed as key intermediates to produce new spiro compounds via novel synthetic approaches.

## 4. EXPERIMENTAL SECTION

**General Information.** Reagents and solvents were purchased from Sigma-Aldrich and purified by standard procedures when required. $^{1}$H NMR spectra were recorded on a Varian Inova 300 (300 MHz) or Bruker 500 (500 MHz) spectrometer. The chemical shifts ($\delta$) are reported in parts per million using tetramethylsilane as an internal standard ($CDCl_3$ at 7.26 ppm). Proton-decoupled $^{13}$C NMR spectra were recorded on a Varian Inova 300 (75 MHz) or Bruker 500 (125 MHz) spectrometer and are reported in parts per million relative to the residual solvent peak ($CDCl_3$ at 77.2 ppm). GC/MS analysis were recorded using a GCM-QP2010SE instrument (Shimadzu) with low-resolution electron impact (EI, 70 eV) equipped with an RTX-5MS capillary column. GC/MS conditions: injector, 260 °C; detector, 110 °C; pressure, 100 kPa; column temperature, from 80 to 280 °C at 1 °C/min. IR spectra were recorded using a PerkinElmer Frontier spectrometer. High-resolution mass spectra were


https://dx.doi.org/10.1021/acs.oprd.0c00057
Org. Process Res. Dev. XXXX, XXX, XXX−XXX

A)

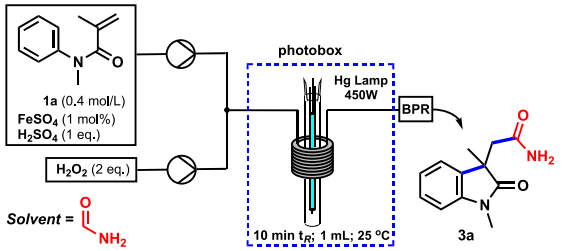


| Control | $FeSO_4$ | $H_2O_{2\ aq}$ | UV light | Product [%] |
|---|---|---|---|---|
| 1 | 1 mol % | 0.4 mol/L | yes | >99 |
| 2 | 1 mol % | 0.4 mol/L | no | trace |
| 3 | - | 0.4 mol/L | yes | 0 |

B)

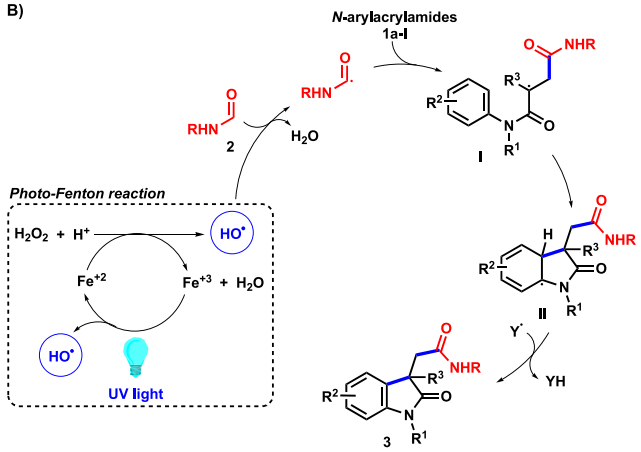


**Figure 4.** Control experiments and possible mechanism.

obtained on a Bruker Daltonics MicroToF spectrometer using electrospray ionization–time of flight (ESI-TOF) techniques.

*N*-Arylacrylamides **1a–l** were prepared according to the literature protocols (for more details, see the Supporting Information).[14,18]

**Setup for the Photochemical Flow Reactor.** The photochemical reactor consisted of a UV lamp (450 W Hg lamp) that was inserted into a filter sleeve (glass type: Pyrex). Both the UV lamp and filter sleeve were inserted into a quartz immersion well. A tube reactor (reactor volume = 1 mL; high-purity perfluoroalkoxyalkane (HPFA) tubing; 19 mm × 9 mm × 2.21 m) was wrapped around the quartz immersion well. A water bath was employed to control the reaction temperature. A back-pressure regulator (BPR) set at 75 psi was connected. The entire system was placed inside an aluminum-foil-covered box called the "photobox". The photobox had a size of 46 cm × 64 cm × 44 cm ($W \times H \times D$) and fit conveniently onto a lab bench. The tube reactor was connected to the syringes via a Y-adapter. One syringe was loaded with solution 1 and the other with solution 2. A syringe pump was used to infuse the two solutions through the photochemical reactor.

**General Procedure for the Photo-Fenton Process in Formamide under Continuous Flow Conditions.** Two solutions containing the chemicals were prepared in volumetric flasks as follows:

Solution 1: To a 10 mL volumetric flask were added *N*-arylacrylamide **1** (0.4 M) and $FeSO_4 \cdot 7H_2O$ (1 mol %), and the volume was completed with formamide. Nitrogen gas was bubbled over 5 min, and then $H_2SO_4$ (0.4 M) was added.

Solution 2: To a 10 mL volumetric flask was added aqueous $H_2O_2$ (30 wt % in $H_2O$; 0.8 M), and the volume was completed with formamide. Nitrogen gas was bubbled over 5 min.

*Note:* Because of the solubility of some starting materials, it was necessary to decrease their concentrations in solution 1 (**1e**, 0.04 M; **1f** and **1i**, 0.136 M; **1h**, 0.2 M). Also, *tert*-butanol was used as a cosolvent (2% v/v).

**Scheme 2. Synthesis of New Spiro Compounds**[a]

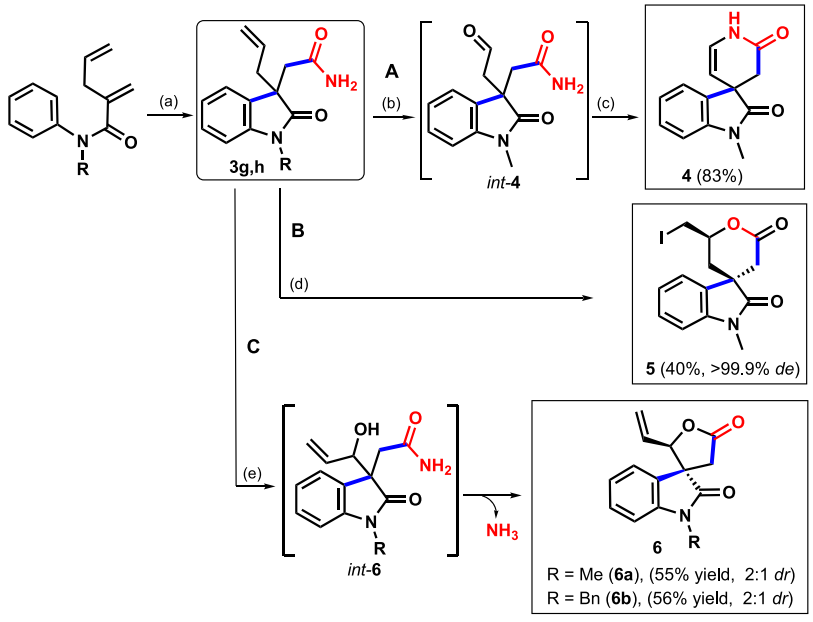


[a]Reaction conditions: (a) continuous photo-Fenton process in formamide, $t_R$ = 10 min (**3g**, 77%; **3h**, 97%); (b) $RuCl_3$ (3.5 mol %), $NaIO_4$, ACN/$H_2O$, rt, 2 h; (c) Dean–Stark, toluene, 4 h; (d) $I_2$, THF, $H_2O$, 1.5 h, 0 °C; (e) TBHP (70% aqueous solution), $SeO_2$, reflux, 96 h.



https://dx.doi.org/10.1021/acs.oprd.0c00057
Org. Process Res. Dev. XXXX, XXX, XXX–XXX

**Operational Conditions for the Photochemical Flow Reactor.** Considering two syringes and the reactor volume (1 mL), the injection flow rate was 50 μL/min for a residence time of 10 min. For reactor equilibration, both solutions were infused for 3 times the desired residence time, and the reaction effluent was discharged. After the reactor equilibration, the reaction effluent was collected in a single flask. The isolated yield was measured after continuous production of the desired oxindole for 1.5 h. For example, the reaction effluent (7 mL) was collected in a single flask, and this crude material was purified by flash column chromatography as described below.

Each reaction was monitored, and every 10 min one sample of the reaction effluent was collected for analysis by TLC and GC/MS. This protocol was repeated three times. For sample extraction, a saturated aqueous solution of sodium bicarbonate (0.5 mL) and $CHCl_3$ (2 mL) were added to the flask. The resulting mixture was stirred, and the organic layer was removed. In the same flask, the aqueous layer was washed with $CHCl_3$ (2 mL). The combined organic layers were dried over $MgSO_4$, filtered, and analyzed by TLC and GC/MS.

**Typical Procedure for Purification of Oxindoles 3a−j.** The reaction effluent (7 mL) was used without quenching to load a glass chromatography column (silica gel; diameter = 4 cm, length = 20 cm). This glass column was very efficient for separation of the oxindole and formamide. A 9:1 $CHCl_3$/MeOH mixture was used as the eluent.

To recycle formamide, prior to chromatography a simple vacuum distillation was used.

*2-(1,3-Dimethyl-2-oxoindolin-3-yl)acetamide (**3a**).*[14] Yield = 99%, 0.303 g; $R_f$ = 0.39 (9:1 $CHCl_3$/MeOH); $^1$H NMR ($CDCl_3$, 500 MHz) $\delta$ 1.45 (s, 3H), 2.68 (d, 1H, $J$ = 15 Hz), 2.82 (d, 1H, $J$ = 15 Hz), 3.24 (s, 3H), 5.35 (br s, 1H), 6.42 (br s, 1H), 6.86 (d, 1H, $J$ = 5 Hz), 7.07−7.10 (m, 1H), 7.27−7.30 (m, 2H) ppm; $^{13}$C NMR ($CDCl_3$, 125 MHz) $\delta$ 23.7, 26.5, 43.4, 46.1, 108.5, 122.8, 123.0, 128.3, 133.4, 142.9, 171.6, 180.7 ppm; IR (ATR) $\nu_{max}$ 3383, 3202, 2967, 1713, 1699, 1680, 1614, 1495 cm$^{-1}$; MS (EI$^+$) $m/z$ (relative intensity) 218 ($M^+$, 40), 160 (100).

*2-(5-Methyl-1,3-dimethyl-2-oxoindolin-3-yl)acetamide (**3b**).*[14] Yield = 47%, 0.110 g (from 5 mL of output solution); $R_f$ = 0.39 (9:1 $CHCl_3$/MeOH); $^1$H NMR ($CDCl_3$, 500 MHz) $\delta$ 1.45 (s, 3H), 2.34 (s, 3H), 2.68 (d, 1H, $J$ = 15 Hz), 2.80 (d, 1H, $J$ = 15 Hz), 3.22 (s, 3H), 5.21 (br s, 1H), 6.55 (br s, 1H), 6.75 (d, 1H, $J$ = 10 Hz), 7.07−7.09 (m, 2H) ppm; $^{13}$C NMR ($CDCl_3$, 125 MHz) $\delta$ 21.3, 23.6, 26.6, 43.6, 46.1, 108.3, 123.7, 128.7, 132.7, 133.4, 140.5, 171.6, 180.7 ppm; IR (ATR) $\nu_{max}$ 3381, 3189, 2963, 1707, 1695, 1683, 1606, 1502 cm$^{-1}$; MS (EI$^+$) $m/z$ (relative intensity) 232 ($M^+$, 38), 174 (100).

*2-(5-Methoxy-1,3-dimethyl-2-oxoindolin-3-yl)acetamide (**3c**).*[14] Yield = 74%, 0.258 g; $R_f$ = 0.28 (9:1 $CHCl_3$/MeOH); $^1$H NMR ($CDCl_3$, 500 MHz) $\delta$ 1.45 (s, 3H), 2.68 (d, 1H, $J$ = 15 Hz), 2.79 (d, 1H, $J$ = 15 Hz), 3.22 (s, 3H), 3.79 (s, 3H), 5.30 (br s, 1H), 6.58 (br s, 1H), 6.76 (d, 1H, $J$ = 10 Hz), 6.81 (dd, 1H, $J$ = 10 Hz, $J$ = 2.5 Hz), 6.90 (d, 1H, $J$ = 2.5 Hz) ppm; $^{13}$C NMR ($CDCl_3$, 125 MHz) $\delta$ 23.5, 26.6, 43.6, 46.4, 55.9, 108.8, 110.5, 112.6, 134.8, 136.3, 156.5, 171.5, 180.4 ppm; MS (EI$^+$) $m/z$ (relative intensity) 248 ($M^+$, 82), 190 (100).

*2-(5-Chloro-1,3-dimethyl-2-oxoindolin-3-yl)acetamide (**3d**).*[14] Yield = 86%, 0.306 g; $R_f$ = 0.49 (9:1 $CHCl_3$/MeOH); $^1$H NMR (DMSO-$d_6$, 300 MHz) $\delta$ 1.20 (s, 3H), 2.61 (d, 1H, $J$ = 15 Hz), 2.80 (d, 1H, $J$ = 15 Hz), 3.09 (s, 3H), 6.59 (br s, 1H), 6.97 (d, 1H, $J$ = 9 Hz), 7.22 (br s, 1H), 7.26 (dd, 1H, $J$ = 9 Hz, $J$ = 2 Hz), 7.39 (d, 1H, $J$ = 2 Hz) ppm; $^{13}$C NMR (DMSO-$d_6$, 75 MHz) $\delta$ 24.1, 26.2, 41.9, 45.3, 109.3, 122.7, 125.6, 127.1, 135.9, 142.6, 170.5, 179.3 ppm; IR (KBr) $\nu_{max}$ 3370, 3191, 2965, 1702, 1681, 1612, 1495, 1081, 1054 cm$^{-1}$; MS (EI$^+$) $m/z$ (relative intensity) 252 ($M^+$, 42), 194 (100).

*2-(7-Phenyl-1,3-dimethyl-2-oxoindolin-3-yl)acetamide (**3e**).*[14] Yield = 60%, 0.026 g (from 4.3 mL of output solution, 0.02 M); $R_f$ = 0.39 (9:1 $CHCl_3$/MeOH); $^1$H NMR ($CDCl_3$, 500 MHz) $\delta$ 1.50 (s, 3H), 2.74 (d, 1H, $J$ = 15 Hz), 2.76 (s, 3H), 2.87 (d, 1H, $J$ = 15 Hz), 5.32 (br s, 1H), 6.53 (br s, 1H), 7.08−7.12 (m, 2H), 7.34−7.41 (m, 6H) ppm; $^{13}$C NMR ($CDCl_3$, 125 MHz) $\delta$ 24.0, 30.6, 43.9, 45.4, 121.8, 122.4, 125.9, 127.8, 128.8, 130.0, 131.4, 134.4, 138.9, 139.8, 171.5, 181.8 ppm; IR (ATR) $\nu_{max}$ 3339, 3201, 2963, 1699, 1679, 1613, 1458 cm$^{-1}$; MS (EI$^+$) $m/z$ (relative intensity) 294 ($M^+$, 46), 236 (100).

*2-(3-Benzyl-1-methyl-2-oxoindolin-3-yl)acetamide (**3f**).* Yield = 82%, 0.169 g (from 7 mL of output solution, 0.068 M); $R_f$ = 0.31 (9:1 $CHCl_3$/MeOH); $^1$H NMR ($CDCl_3$, 500 MHz) $\delta$ 2.79 (d, 1H, $J$ = 15 Hz), 2.96 (s, 3H), 2.98 (d, 1H, $J$ = 15 Hz), 3.09 (d, 1H, $J$ = 15 Hz), 3.15 (d, 1H, $J$ = 15 Hz), 5.36 (br s, 1H), 6.30 (br s, 1H), 6.58 (d, 1H, $J$ = 10 Hz), 6.78 (d, 2H, $J$ = 10 Hz), 7.02−7.09 (m, 4H), 7.18 (dd, 1H, $J$ = 10 Hz, $J$ = 1 Hz), 7.21 (d, 1H, $J$ = 5 Hz) ppm; $^{13}$C NMR ($CDCl_3$, 125 MHz) $\delta$ 26.1, 42.3, 43.7, 52.1, 108.2, 122.6, 123.8, 126.9, 127.6, 128.5, 130.0, 130.3, 135.0, 143.6, 171.3, 179.2 ppm; IR (ATR) $\nu_{max}$ 3391, 3198, 2936, 1714, 1682, 1670, 1613, 1495 cm$^{-1}$; MS (EI$^+$) $m/z$ (relative intensity) 294 ($M^+$, 46), 160 (100).

*2-(3-Allyl-1-methyl-2-oxoindolin-3-yl)acetamide (**3g**).*[19] Yield = 77%, 0.263 g; $R_f$ = 0.35 (9:1 $CHCl_3$/MeOH); $^1$H NMR ($CDCl_3$, 500 MHz) $\delta$ 2.55−2.64 (m, 2H), 2.72 (d, 1H, $J$ = 15 Hz), 2.86 (d, 1H, $J$ = 15 Hz), 3.23 (s, 3H), 4.95−5.03 (m, 2H), 5.17 (br s, 1H), 5.38−5.46 (m, 1H), 6.26 (br s, 1H), 6.85 (d, 1H, $J$ = 10 Hz), 7.08 (td, 1H, $J$ = 8 Hz, $J$ = 1 Hz), 7.25−7.27 (m, 1H), 7.29 (td, 1H, $J$ = 8 Hz, $J$ = 1.5 Hz) ppm; $^{13}$C NMR ($CDCl_3$, 125 MHz) $\delta$ 26.4, 41.7, 42.3, 50.3, 108.4, 119.7, 122.8, 123.4, 128.5, 131.0, 131.6, 143.6, 171.3, 179.5 ppm; IR (ATR) $\nu_{max}$ 3405, 3203, 2963, 1717, 1681, 1667, 1631, 1613, 1495 cm$^{-1}$; MS (EI$^+$) $m/z$ (relative intensity) 244 ($M^+$, 40), 160 (100).

*2-(3-Allyl-1-benzyl-2-oxoindolin-3-yl)acetamide (**3h**).* Yield = 97%, 0.218 g (from 7 mL of output solution, 0.1 M); $R_f$ = 0.38 (9:1 $CHCl_3$/MeOH); $^1$H NMR ($CDCl_3$, 500 MHz) $\delta$ 2.60−2.69 (m, 2H), 2.77 (d, 1H, $J$ = 15 Hz), 2.92 (d, 1H, $J$ = 15 Hz), 4.86 (d, 1H, $J$ = 15 Hz), 4.96−5.07 (m, 3H), 5.13 (br s, 1H), 5.39−5.47 (m, 1H), 6.14 (br s, 1H), 6.72 (d, 1H, $J$ = 8 Hz), 7.05 (td, 1H, $J$ = 8 Hz, $J$ = 1 Hz), 7.17 (td, 1H, $J$ = 8 Hz, $J$ = 1 Hz), 7.23−7.33 (m, 6H) ppm; $^{13}$C NMR ($CDCl_3$, 125 MHz) $\delta$ 42.0, 42.4, 44.1, 50.3, 109.4, 119.9, 122.8, 123.4, 127.4, 127.7, 128.4, 128.8, 130.9, 131.6, 135.9, 142.8, 171.2, 179.6 ppm; MS (EI$^+$) $m/z$ (relative intensity) 320 ($M^+$, 10), 91 (100); HRMS (ESI-TOF) calcd for $C_{20}H_{21}N_2O_2$ $[M + H]^+$ 321.1603, found (M + 1) 321.1601.

*2-(1-Benzyl-3-methyl-2-oxoindolin-3-yl)acetamide (**3i**).* Yield = 90%, 0.127 g (from 5 mL of output solution, 0.068 M); $R_f$ = 0.39 (9:1 $CHCl_3$/MeOH); $^1$H NMR ($CDCl_3$, 500 MHz) $\delta$ 1.49 (s, 3H), 2.75 (d, 1H, $J$ = 15 Hz), 2.89 (d, 1H, $J$ = 15 Hz), 4.94 (s, 2H), 5.36 (br s, 1H), 6.28 (br s, 1H), 6.73 (d, 1H, $J$ = 8 Hz), 7.04 (td, 1H, $J$ = 8 Hz, $J$ = 1 Hz), 7.16 (td, 1H, $J$ = 8 Hz, $J$ = 1.5 Hz), 7.24−7.28 (m, 2H), 7.30−7.34 (m, 4H) ppm; $^{13}$C NMR ($CDCl_3$, 125 MHz) $\delta$ 24.2, 43.4, 44.0, 46.2, 109.6, 122.9, 123.1, 127.3, 127.8, 128.3, 128.9, 133.3, 135.9,


https://dx.doi.org/10.1021/acs.oprd.0c00057
Org. Process Res. Dev. XXXX, XXX, XXX−XXX

142.1, 171.4, 180.8 ppm; IR (ATR) $\nu_{max}$ 3398, 3196, 2965, 1707, 1681, 1612, 1491 $cm^{-1}$; MS ($EI^+$) $m/z$ (relative intensity) 294 ($M^+$, 18), 91 (100).

*2-(6-Methoxy-1,3-dimethyl-2-oxoindolin-3-yl)acetamide (**3j**).* Yield = 81%, 0.280 g; $R_f$ = 0.39 (9:1 $CHCl_3$/MeOH).

Major isomer: $^1H$ NMR ($CDCl_3$, 500 MHz) $\delta$ 1.45 (s, 3H), 2.92 (d, 1H, $J$ = 15 Hz), 2.96 (d, 1H, $J$ = 15 Hz), 3.21 (s, 3H), 3.86 (s, 3H), 5.39 (br s, 1H), 6.15 (br s, 1H), 6.52 (d, 1H, $J$ = 8 Hz), 6.62 (d, 1H, $J$ = 8 Hz), 7.23 (t, 1H, $J$ = 8 Hz) ppm; $^{13}C$ NMR ($CDCl_3$, 125 MHz) $\delta$ 21.7, 26.7, 41.5, 46.5, 55.6, 101.9, 106.1, 123.5, 129.5, 144.5, 155.9, 172.1, 180.8 ppm.

Minor isomer: $^1H$ NMR ($CDCl_3$, 500 MHz) $\delta$ 1.40 (s, 3H), 2.66 (d, 1H, $J$ = 15 Hz), 2.76 (d, 1H, $J$ = 15 Hz), 3.21 (s, 3H), 3.82 (s, 3H), 5.48 (br s, 1H), 6.36 (br s, 1H), 6.44 (d, 1H, $J$ = 2 Hz), 6.57 (dd, 1H, $J$ = 8 Hz, $J$ = 2 Hz), 7.16 (d, 1H, $J$ = 8 Hz) ppm; $^{13}C$ NMR ($CDCl_3$, 125 MHz) $\delta$ 23.8, 26.5, 43.6, 45.7, 55.6, 96.6, 106.7, 118.5, 125.2, 144.2, 160.3, 171.7, 181.2 ppm.

IR (ATR) $\nu_{max}$ 3400, 3206, 2966, 1701, 1665, 1627, 1608, 1475, 1260, 1071 $cm^{-1}$; MS ($EI^+$) $m/z$ (relative intensity) 248 ($M^+$, 43), 190 (100); HRMS (ESI-TOF) calcd for $C_{13}H_{17}N_2O_3$ $[M + H]^+$ 249.1239, found (M + 1) 249.1233.

**Typical Procedure for the Purification of Oxindoles 3k–n.** The reaction effluent (7 mL) was quenched with a saturated aqueous solution of $NaHCO_3$ to pH 7. Also, 2 equiv of $Na_2SO_3$ was added. The resulting mixture was filtered through a short pad of silica gel (MeOH), and then methanol and *N*-methylformamide were removed by reduced-pressure distillation. The resulting crude mixture was dissolved using chloroform and filtered to remove any insoluble material. The solvent was removed under reduced pressure, and the crude mixture was used to load a glass chromatography column (silica gel; diameter = 4 cm, length = 20 cm). A 95:5 $CHCl_3$/MeOH mixture was used as the eluent.

*2-(1,3-Dimethyl-2-oxoindolin-3-yl)-N-methylacetamide (**3k**).*[14] Yield = 89%, 0.289 g; $R_f$ = 0.45 (95:5 $CHCl_3$/MeOH); $^1H$ NMR ($CDCl_3$, 500 MHz) $\delta$ 1.42 (s, 3H), 2.66 (d, 1H, $J$ = 15 Hz), 2.67 (d, 3H, $J$ = 5 Hz), 2.78 (d, 1H, $J$ = 15 Hz), 3.25 (s, 3H), 6.36 (br s, 1H), 6.86 (d, 1H, $J$ = 8 Hz), 7.07 (td, 1H, $J$ = 8 Hz, $J$ = 1 Hz), 7.25–7.29 (m, 2H) ppm; $^{13}C$ NMR ($CDCl_3$, 125 MHz) $\delta$ 23.7, 26.3, 26.5, 43.7, 46.2, 108.4, 122.8, 122.9, 128.2, 133.6, 143.0, 169.9, 180.9 ppm; IR (ATR) $\nu_{max}$ 3323, 2965, 1713, 1656, 1613, 1495 $cm^{-1}$; MS ($EI^+$) $m/z$ (relative intensity) 232 ($M^+$, 40), 160 (100).

*N-Methyl-2-(1,3,5-trimethyl-2-oxoindolin-3-yl)-N-methylacetamide (**3l**).*[14] Yield = 42%, 0.143 g; $R_f$ = 0.45 (95:5 $CHCl_3$/MeOH); $^1H$ NMR ($CDCl_3$, 500 MHz) $\delta$ 1.41 (s, 3H), 2.34 (s, 3H), 2.64 (d, 1H, $J$ = 15 Hz), 2.72 (d, 3H, $J$ = 5 Hz), 2.75 (d, 1H, $J$ = 15 Hz), 3.22 (s, 3H), 6.45 (br s, 1H), 6.75 (d, 1H, $J$ = 8 Hz), 7.06–7.08 (m, 2H) ppm; $^{13}C$ NMR ($CDCl_3$, 125 MHz) $\delta$ 21.3, 23.6, 26.3, 26.5, 43.8, 46.2, 108.2, 123.7, 128.5, 132.5, 133.7, 140.4, 169.9, 180.8 ppm; IR (ATR) $\nu_{max}$ 3327, 2963, 1714, 1687, 1649, 1602, 1501 $cm^{-1}$; MS ($EI^+$) $m/z$ (relative intensity) 246 ($M^+$, 55), 174 (100).

*2-(5-Methoxy-1,3-dimethyl-2-oxoindolin-3-yl)-N-methylacetamide (**3m**).*[14] Yield = 59%, 0.154 g (from 5 mL of output solution); $R_f$ = 0.39 (95:5 $CHCl_3$/MeOH); $^1H$ NMR ($CDCl_3$, 500 MHz) $\delta$ 1.42 (s, 3H), 2.64 (d, 1H, $J$ = 15 Hz), 2.72 (d, 3H, $J$ = 5 Hz), 2.76 (d, 1H, $J$ = 15 Hz), 3.22 (s, 3H), 3.79 (s, 3H), 6.47 (br s, 1H), 6.76 (d, 1H, $J$ = 8.5 Hz), 6.80 (dd, 1H, $J$ = 8.5 Hz, $J$ = 2.5 Hz), 6.89 (d, 1H, $J$ = 2.5 Hz) ppm; $^{13}C$ NMR ($CDCl_3$, 125 MHz) $\delta$ 23.6, 26.3, 26.5, 43.6, 46.5, 55.9, 108.7, 110.4, 112.3, 135.0, 136.4, 156.3, 169.8, 180.5 ppm; IR (ATR) $\nu_{max}$ 3328, 2960, 1707, 1684, 1650, 1599, 1498, 1294, 1041 $cm^{-1}$; MS ($EI^+$) $m/z$ (relative intensity) 262 ($M^+$, 95), 190 (100).

*2-(3-Benzyl-1-methyl-2-oxoindolin-3-yl)-N-methylacetamide (**3n**).* Yield = 58%, 0.041 g (from 3.4 mL of output solution, 0.068 M); $R_f$ = 0.47 (95:5 $CHCl_3$/MeOH); $^1H$ NMR ($CDCl_3$, 500 MHz) $\delta$ 2.69 (d, 3H, $J$ = 5 Hz), 2.77 (d, 1H, $J$ = 15 Hz), 2.95 (d, 1H, $J$ = 15 Hz), 2.97 (s, 3H), 3.12 (d, 2H, $J$ = 5 Hz), 6.21 (br s, 1H), 6.58 (d, 1H, $J$ = 8 Hz), 6.77–6.79 (m, 2H), 7.01–7.06 (m, 4H), 7.16–7.21 (m, 2H) ppm; $^{13}C$ NMR ($CDCl_3$, 125 MHz) $\delta$ 26.1, 26.4, 42.7, 43.6, 52.1, 108.1, 122.4, 123.8, 126.8, 127.6, 128.4, 130.1, 130.6, 135.1, 143.6, 169.7, 179.4 ppm; MS ($EI^+$) $m/z$ (relative intensity) 308 ($M^+$, 12), 160 (100).

**Synthesis of Spiro[oxindole-3,4-dihydropyridin-2-one] 4 via Oxidative Cleavage of the C=C Bond.** **Step 1:** An aqueous solution of $RuCl_3$ (500 $\mu$L, 0.035 mmol, 3.5 mol %) was added to a solution of oxindole **3g** (122.1 mg, 0.5 mmol) in 6:1 acetonitrile/water (3.5 mL). Then $NaIO_4$ (213.9 mg, 1.0 mmol) was added portionwise over a period of 5 min at room temperature. The resulting mixture was stirred for 2 h. The reaction was quenched with a saturated aqueous solution of $Na_2S_2O_3$ (10 mL) and extracted with EtOAc (3 × 10 mL). The combined organic layers were washed with water (20 mL) and brine (20 mL), dried over $MgSO_4$, and concentrated under reduced pressure. The crude material containing the desired compound *int*-**4** was used in the next reaction without further purification. **Step 2:** The crude material containing compound *int*-**4** (0.5 mmol) was dissolved in toluene. The resulting mixture was stirred in a Dean–Stark apparatus and monitored by TLC. After 4 h, the solvent was removed under reduced pressure. The crude mixture was purified by flash column chromatography on silica gel (9:1 $CHCl_3$/MeOH).

*1-Methyl-1′H-spiro[indoline-3,4′-pyridine]-2,2′(3′H)-dione (**4**).* Yield = 83%; $R_f$ = 0.40 (9:1 $CHCl_3$/MeOH); $^1H$ NMR ($CDCl_3$, 500 MHz) $\delta$ 2.62 (d, 1H, $J$ = 16.4 Hz), 3.03 (d, 1H, $J$ = 16.4 Hz), 3.23 (s, 3H), 4.88 (d, 1H, $J$ = 7.7 Hz), 6.42 (dd, 1H, $J$ = 7.7 Hz, $J$ = 1.2 Hz), 6.86 (d, 1H, $J$ = 7.8 Hz), 7.07 (td, 1H, $J$ = 7.6 Hz, $J$ = 1 Hz), 7.15 (br s, 1H), 7.27 (d, 1H, $J$ = 7.7 Hz), 7.32 (td, 1H, $J$ = 7.7 Hz, $J$ = 1.2 Hz); $^{13}C$ NMR ($CDCl_3$, 125 MHz) $\delta$ 26.6, 38.7, 48.3, 105.1, 108.5, 123.3, 123.4, 127.7, 129.0, 132.1, 142.4, 168.5, 177.7 ppm; IR (KBr) $\nu_{max}$ 3272, 1711, 1656, 1611, 1470, 1349, 1090, 697 $cm^{-1}$; MS ($EI^+$) $m/z$ (relative intensity) 130 (25), 199 (52), 213 (8), 227 (50, $M^+$), 228 (100, $M^+$), 229 ($M^+$, 15); HRMS calcd for $C_{13}H_{12}N_2O_2$ $[M + Na]^+$ 251.0796, found (M + 23) 251.0795.

**Synthesis of Spiro[oxindole-δ-lactone] 5 via Iodolactonization.** $I_2$ (380.7 mg, 1.5 mmol) was added portionwise over a period of 10 min to a solution of oxindole **3g** (122.1 mg, 0.5 mmol) in 1:1 tetrahydrofuran/water (4 mL) cooled to 0 °C. After 1.5 h at 0 °C, the reaction was quenched with a saturated aqueous solution of $Na_2S_2O_3$ (10 mL). The mixture was extracted with $CH_2Cl_2$ (3 × 10 mL). The combined organic layers were washed with brine (20 mL), dried over $MgSO_4$, and concentrated under reduced pressure. The mixture was purified by flash column chromatography on silica gel (1:1 EtOAc/hexane).

*2′-(Iodomethyl)-1-methyl-2′,3′-dihydrospiro[indoline-3,4′-pyran]-2,6′(5′H)-dione (**5**).* Yield = 40%; $R_f$ = 0.51 (1:1 EtOAc/hexane); $^1H$ NMR ($CDCl_3$, 500 MHz) $\delta$ 2.06–2.02 (m, 1H), 2.17–2.23 (m, 1H), 2.53 (dd, 1H, $J$ = 17.4 Hz, $J$ = 2.3 Hz), 2.95 (d, 1H, $J$ = 17.4 Hz), 3.26 (s, 3H), 3.39–3.46 (m, 2H), 4.68–4.74 (m, 1H), 6.94 (d, 1H, $J$ = 7.8 Hz), 7.12 (t,


https://dx.doi.org/10.1021/acs.oprd.0c00057
Org. Process Res. Dev. XXXX, XXX, XXX–XXX

1H, $J$ = 7.6 Hz), 7.24 (d, 1H, $J$ = 7.2 Hz), 7.38 (td, 1H, $J$ = 7.8 Hz, $J$ = 1 Hz); $^{13}$C NMR ($CDCl_3$, 125 MHz) $\delta$ 7.0, 26.7, 36.1, 36.2, 45.5, 75.7, 109.1, 123.3, 123.4, 129.4, 130.5, 142.8, 168.0, 176.8 ppm; IR (KBr) $\nu_{max}$ 1747, 1712, 1612, 1494, 1470, 1376, 1354, 754 cm$^{-1}$; MS (EI$^+$) $m/z$ (relative intensity) 130 (35), 160 (100), 244 (45), 371 (11, M$^+$), 372 (M$^+$, 2); HRMS calcd for $C_{13}H_{12}N_2O_2$ [M + Na]$^+$ 393.9916, found (M + 23) 393.9915.

**Synthesis of Spiro[oxindole-γ-lactones] 6a and 6b via Allylic Oxidation and Lactonization.** TBHP (70% aqueous solution; 3.9 mmol) and $SeO_2$ (1.6 mmol) were added to a solution of the oxindole (**3g** or **3h**) (0.8 mmol) in $CH_2Cl_2$ (25 mL). The resulting mixture was stirred under reflux for 96 h. The reaction was quenched with a 1 M aqueous solution of HCl (10 mL). The mixture was extracted with $CHCl_3$ (3 × 10 mL). The combined organic layers were dried over $MgSO_4$ and concentrated under reduced pressure. The crude material was purified by flash column chromatography on silica gel (7:3 hexanes/EtOAc). The diastereoisomers were separated and fully characterized.

*1′-Methyl-2-vinyl-2H-spiro[furan-3,3′-indoline]-2′,5(4H)-dione (**6a**).* Yield = 55%. Spectral data for the isolated diastereomers:

Major diastereomer: $R_f$ = 0.34 (7:3 hexanes/EtOAc); $^1$H NMR ($CDCl_3$, 500 MHz) $\delta$ 2.69 (d, 1H, $J$ = 17.1 Hz), 3.25 (s, 3H), 3.32 (d, 1H, $J$ = 17.1 Hz), 5.11 (d, 1H, $J$ = 9.7 Hz), 5.15 (m, 1H), 5.34 (dd, 1H, $J$ = 17.5 Hz, $J$ = 1.8 Hz), 5.37−5.44 (m, 1H), 6.89 (d, 1H, $J$ = 7.9 Hz), 7.11 (td, 1H, $J$ = 7.6 Hz, $J$ = 0.9 Hz), 7.24 (d, 1H, $J$ = 7.4 Hz), 7.36 (td, 1H, $J$ = 7.8 Hz, $J$ = 1.2 Hz); $^{13}$C NMR ($CDCl_3$, 125 MHz) $\delta$ 39.6, 44.2, 55.6, 85.6, 108.8, 120.5, 123.3, 123.8, 127.8, 129.5, 130.4, 142.9, 173.7, 174.2 ppm; IR (KBr) $\nu_{max}$ 1790, 1715, 1614, 1495, 1472 1378, 1354, 755 cm$^{-1}$; MS (EI$^+$) $m/z$ (relative intensity) 130 (44), 159 (100), 187 (18), 243 (M$^+$, 5); HRMS calcd for $C_{14}H_{13}NO_3$ [M + H]$^+$ 244.0974, found (M + 1) 244.0961.

Minor diastereomer: $R_f$ = 0.29 (7:3 hexanes/EtOAc); $^1$H NMR ($CDCl_3$, 500 MHz) $\delta$ 2.92 (d, 1H, $J$ = 17.4 Hz), 3.01 (d, 1H, $J$ = 17.4 Hz), 3.19 (s, 3H), 4.97 (d, 1H, $J$ = 7.0 Hz), 5.15−5.21 (m, 2H), 5.86−5.89 (m, 1H), 6.86 (d, 1H, $J$ = 7.8 Hz), 7.15 (td, 1H, $J$ = 7.6 Hz, $J$ = 0.9 Hz), 7.33 (d, 1H, $J$ = 7.4 Hz), 7.36 (td, 1H, $J$ = 7.8 Hz, $J$ = 1.1 Hz) ppm; $^{13}$C NMR ($CDCl_3$, 125 MHz) $\delta$ 25.3, 37.1, 53.4, 85.1, 107.6, 121.5, 119.4, 122.3, 126.2, 128.7, 129.3, 142.9, 172.3, 174.0 ppm; MS (EI$^+$) $m/z$ (relative intensity) 130 (44), 159 (100), 187 (18), 243 (M$^+$, 5).

*1′-Benzyl-2-vinyl-2H-spiro[furan-3,3′-indoline]-2′,5(4H)-dione (**6b**).* Yield = 56%. Spectral data for the isolated diastereomers:

Major diastereomer: $R_f$ = 0.57 (7:3 hexanes/EtOAc); $^1$H NMR ($CDCl_3$, 500 MHz) $\delta$ 2.73 (d, 1H, $J$ = 17.0 Hz), 3.39 (d, 1H, $J$ = 17.0 Hz), 4.76 (d, 1H, $J$ = 15.7 Hz), 5.09 (d, 1H, $J$ = 15.7 Hz), 5.12−5.14 (m, 1H), 5.21 (d, 1H, $J$ = 6.7 Hz), 5.36 (dd, 1H, $J$ = 17.2 Hz, $J$ = 1.9 Hz), 5.39−5.46 (m, 1H), 6.78 (d, 1H, $J$ = 7.8 Hz), 7.08 (td, 1H, $J$ = 7.7 Hz, $J$ = 1.0 Hz), 7.22−7.24 (m, 2H), 7.27−7.32 (m, 5H); $^{13}$C NMR ($CDCl_3$, 125 MHz) $\delta$ 39.6, 44.2, 55.7, 85.9, 109.8, 120.9, 123.3, 123.8, 127.2, 127.8, 127.9, 128.9, 129.4, 130.6, 135.1, 142.1, 173.5, 174.4 ppm; IR (KBr) $\nu_{max}$ 1791, 1717, 1614, 1490, 1468, 1455, 1381, 754 cm$^{-1}$; MS (EI$^+$) $m/z$ (relative intensity) 319 (M$^+$, 2), 91 (100); HRMS calcd for $C_{20}H_{17}NO_3$ [M + H]$^+$ 320.1287, found (M + 1) 320.1274.

Minor diastereomer: $R_f$ = 0.44 (7:3 hexanes/EtOAc); $^1$H NMR ($CDCl_3$, 500 MHz) $\delta$ 2.98 (d, 1H, $J$ = 17.4 Hz), 3.05 (d, 1H, $J$ = 17.4 Hz), 4.71 (d, 1H, $J$ = 15.6 Hz) 5.00 (d, 1H, $J$ = 7.0 Hz), 5.05 (d, 1H, $J$ = 15.6 Hz), 5.17 (d, 1H, $J$ = 6.8 Hz), 5.20−5.17 (m, 2H), 5.83−5.90 (m, 1H), 6.75 (d, 1H, $J$ = 7.9 Hz), 7.11 (td, 1H, $J$ = 7.6 Hz, $J$ = 1.0 Hz), 7.24 (d, 1H, $J$ = 7.8 Hz), 7.26−7.32 (m, 5H); $^{13}$C NMR ($CDCl_3$, 125 MHz) $\delta$ 38.3, 43.9, 54.5, 86.2, 109.7, 120.6, 122.6, 123.3, 126.9, 127.5, 127.9, 128.8, 129.6, 130.5, 136.3, 143.1, 173.2, 175.3 ppm; MS (EI$^+$) $m/z$ (relative intensity) 319 (M$^+$, 3), 91 (100).

## ■ ASSOCIATED CONTENT

### Supporting Information

The Supporting Information is available free of charge at https://pubs.acs.org/doi/10.1021/acs.oprd.0c00057.

Experimental procedures and characterization data (PDF)

## ■ AUTHOR INFORMATION


### Corresponding Author

**Leandro H. Andrade** − *Institute of Chemistry, University of São Paulo, 05300-080 São Paulo, SP, Brazil*; orcid.org/0000-0001-5975-4980; Email: leandroh@iq.usp.br

### Authors

**Marialy N. Sanabria** − *Institute of Chemistry, University of São Paulo, 05300-080 São Paulo, SP, Brazil*

**Milene M. Hornink** − *Institute of Chemistry, University of São Paulo, 05300-080 São Paulo, SP, Brazil*

**Valquíria G. Correia** − *Institute of Chemistry, University of São Paulo, 05300-080 São Paulo, SP, Brazil*

Complete contact information is available at: https://pubs.acs.org/10.1021/acs.oprd.0c00057


### Notes

The authors declare no competing financial interest.

## ■ ACKNOWLEDGMENTS

We thank the National Council for Scientific and Technological Development (CNPq) (Grants 312751/2018-4 and 141672/2015-3), Coordination for the Improvement of Higher Education Personnel (CAPES), and the São Paulo Research Foundation (FAPESP) (Grants 2017/02854-8 and 2019/10762-1) for financial support.

## ■ REFERENCES

(1) Fenton, H. J. H. Oxidation of Tartaric Acid in Presence of Iron. *J. Chem. Soc., Trans.* **1894**, *65*, 899−910.

(2) For some reviews, see: (a) Neyens, E.; Baeyens, J. A Review of Classic Fenton's Peroxidation as an Advanced Oxidation Technique. *J. Hazard. Mater.* **2003**, *98*, 33−50. (b) Pignatello, J. J.; Oliveros, E.; MacKay, A. Advanced Oxidation Processes for Organic Contaminant Destruction Based on the Fenton Reaction and Related Chemistry. *Crit. Rev. Environ. Sci. Technol.* **2006**, *36*, 1−84. (c) Brillas, E.; Sirés, I.; Oturan, M. A. Electro-Fenton Process and Related Electrochemical Technologies Based on Fenton's Reaction Chemistry. *Chem. Rev.* **2009**, *109*, 6570−6631. (d) Dhakshinamoorthy, A.; Navalon, S.; Alvaro, M.; Garcia, H. Metal Nanoparticles as Heterogeneous Fenton Catalysts. *ChemSusChem* **2012**, *5*, 46−64. (e) Pliego, G.; Zazo, J. A.; Garcia-Muñoz, P.; Munoz, M.; Casas, J. A.; Rodriguez, J. J. Trends in the Intensification of the Fenton Process for Wastewater Treatment: An Overview. *Crit. Rev. Environ. Sci. Technol.* **2015**, *45*, 2611−2692. (f) Clarizia, L.; Russo, D.; Di Somma, I.; Marotta, R.; Andreozzi, R. Homogeneous Photo-Fenton Processes at Near Neutral pH: A Review. *Appl. Catal., B* **2017**, *209*, 358−371. (g) Zhu, Y.; Zhu, R.; Xi, Y.; Zhu, J.; Zhu, G.; He, H. Strategies for Enhancing the

Heterogeneous Fenton Catalytic Reactivity: A Review. *Appl. Catal., B* **2019**, *255*, 117739. (h) Zhang, M.-H.; Dong, H.; Zhao, L.; Wang, D.-X.; Meng, D. A Review on Fenton Process for Organic Wastewater Treatment Based on Optimization Perspective. *Sci. Total Environ.* **2019**, *670*, 110−121.

(3) For some examples, see: (a) Navalon, S.; Martin, R.; Alvaro, M.; Garcia, H. Gold on Diamond Nanoparticles as a Highly Efficient Fenton Catalyst. *Angew. Chem., Int. Ed.* **2010**, *49*, 8403−8407. (b) Navalon, S.; De Miguel, M.; Martin, R.; Alvaro, M.; Garcia, H. Enhancement of the Catalytic Activity of Supported Gold Nanoparticles for the Fenton Reaction by Light. *J. Am. Chem. Soc.* **2011**, *133*, 2218−2226. (c) Xia, M.; Long, M.; Yang, Y.; Chen, C.; Cai, W.; Zhou, B. A Highly Active Bimetallic Oxides Catalyst Supported on Al-containing MCM-41 for Fenton Oxidation of Phenol Solution. *Appl. Catal., B* **2011**, *110*, 118−125. (d) Yang, X. J.; Xu, X. M.; Xu, J.; Han, Y. F. Iron Oxychloride (FeOCl): An Efficient Fenton-Like Catalyst for Producing Hydroxyl Radicals in Degradation of Organic Contaminants. *J. Am. Chem. Soc.* **2013**, *135*, 16058−16061. (e) Liu, Y.; Jin, W.; Zhao, Y.; Zhang, G.; Zhang, W. Enhanced Catalytic Degradation of Methylene Blue by $\alpha$-$Fe_2O_3$/graphene Oxide via Heterogeneous Photo-Fenton Reactions. *Appl. Catal., B* **2017**, *206*, 642−652. (f) Li, X.; Huang, X.; Xi, S.; Miao, S.; Ding, J.; Cai, W.; Liu, S.; Yang, X.; Yang, H.; Gao, J.; Wang, J.; Huang, Y.; Zhang, T.; Liu, B. Single Cobalt Atoms Anchored on Porous N-Doped Graphene with Dual Reaction Sites for Efficient Fenton-like Catalysis. *J. Am. Chem. Soc.* **2018**, *140*, 12469−12475.

(4) (a) Oturan, M. A.; Peiroten, J.; Chartrin, P.; Acher, A. J. Complete Destruction of *p*-Nitrophenol in Aqueous Medium by Electro-Fenton Method. *Environ. Sci. Technol.* **2000**, *34*, 3474−3479. (b) Brillas, E.; Boye, B.; Sirés, I.; Garrido, J. A.; Rodríguez, R. M.; Arias, C.; Cabot, P. L.; Comninellis, C. Electrochemical Destruction of Chlorophenoxy Herbicides by Anodic Oxidation and Electro-Fenton using a Boron-Doped Diamond Electrode. *Electrochim. Acta* **2004**, *49*, 4487−4496. (c) Zhou, M.; Tan, Q.; Wang, Q.; Jiao, Y.; Oturan, N.; Oturan, M. A. Degradation of Organics in Reverse Osmosis Concentrate by Electro-Fenton Process. *J. Hazard. Mater.* **2012**, *215*−*216*, 287−293. (d) Jiang, W. L.; Xia, X.; Han, J. L.; Ding, Y. C.; Haider, M. R.; Wang, A. Graphene Modified Electro-Fenton Catalytic Membrane for *in situ* Degradation of Antibiotic Florfenicol. *Environ. Sci. Technol.* **2018**, *52*, 9972−9982.

(5) (a) Lipczynska-Kochany, E. Hydrogen Peroxide Mediated Photodegradation of Phenol as Studied by a Flash Photolysis/HPLC Technique. *Environ. Pollut.* **1993**, *80*, 147−152. (b) Ruppert, G.; Bauer, R.; Heisler, G. The Photo-Fenton Reaction - an Effective Photochemical Wastewater Treatment Process. *J. Photochem. Photobiol., A* **1993**, *73*, 75−78. (c) Rahim Pouran, S.; Abdul Aziz, A. R.; Wan Daud, W. M. A. Review on the Main Advances in Photo-Fenton Oxidation System for Recalcitrant Wastewaters. *J. Ind. Eng. Chem.* **2015**, *21*, 53−69. (d) Zhang, Y.; Zhang, N.; Wang, T.; Huang, H.; Chen, Y.; Li, Z.; Zou, Z. Heterogeneous Degradation of Organic Contaminants in the Photo-Fenton Reaction Employing Pure Cubic $\beta$-$Fe_2O_3$. *Appl. Catal., B* **2019**, *245*, 410−419.

(6) For some examples of synthetic approaches for oxindoles, see: (a) Ou, W.; Zhang, G.; Wu, J.; Su, C. Photocatalytic Cascade Radical Cyclization Approach to Bioactive Indoline-Alkaloids over Donor−Acceptor Type Conjugated Microporous Polymer. *ACS Catal.* **2019**, *9*, 5178−5183. (b) Li, X.; Han, M.-Y.; Wang, B.; Wang, L.; Wang, M. Visible-Light-Induced Deboronative Alkylarylation of Acrylamides with Organoboronic Acids. *Org. Biomol. Chem.* **2019**, *17*, 6612−6619. (c) Li, Z.; Cui, X.; Niu, L.; Ren, Y.; Bian, M.; Yang, X.; Yang, B.; Yan, Q.; Zhao, J. An Iron(II) Chloride-Promoted Radical Cascade Methylation or $\alpha$-Chloro-$\beta$-methylation of *N*-Arylacrylamides with Dimethyl Sulfoxide. *Adv. Synth. Catal.* **2017**, *359*, 246−249. (d) Correia, V. G.; Abreu, J. C.; Barata, C. A. E.; Andrade, L. H. Iron-Catalyzed Synthesis of Oxindoles: Application to the Preparation of Pyrroloindolines. *Org. Lett.* **2017**, *19*, 1060−1063. (e) Caporaso, R.; Manna, S.; Zinken, S.; Kochnev, A. R.; Lukyanenko, E. R.; Kurkin, A. V.; Antonchick, A. P. Radical Trideuteromethylation with Deuterated Dimethyl Sulfoxide in the Synthesis of Heterocycles and Labelled Building Blocks. *Chem. Commun.* **2016**, *52*, 12486−12489. (f) Tang, Q.; Liu, X.; Liu, S.; Xie, H.; Liu, W.; Zeng, J.; Cheng, P. *N*-(Acyloxy)phthalimides as Tertiary Alkyl Radical Precursors in the Visible Light Photocatalyzed Tandem Radical Cyclization of *N*-Arylacrylamides to 3,3-Dialkyl Substituted Oxindoles. *RSC Adv.* **2015**, *5*, 89009−89014. (g) Xie, J.; Xu, P.; Li, H.; Xue, Q.; Jin, H.; Cheng, Y.; Zhu, C. A Room Temperature Decarboxylation/C−H Functionalization Cascade by Visible-Light Photoredox Catalysis. *Chem. Commun.* **2013**, *49*, 5672−5674.

(7) Manley, P. W.; Bold, G.; Brüggen, J.; Fendrich, G.; Furet, P.; Mestan, J.; Schnell, C.; Stolz, B.; Meyer, T.; Meyhack, B.; Stark, W.; Strauss, A.; Wood, J. Advances in the structural biology, design and clinical development of VEGF-R kinase inhibitors for the treatment of angiogenesis. *Biochim. Biophys. Acta, Proteins Proteomics* **2004**, *1697*, 17−27.

(8) Bramson, H. N.; Corona, J.; Davis, S. T.; Dickerson, S. H.; Edelstein, M.; Frye, S. V.; Gampe, R. T.; Harris, P. A.; Hassell, A.; Holmes, W. D.; Hunter, R. N.; Lackey, K. E.; Lovejoy, B.; Luzzio, M. J.; Montana, V.; Rocque, W. J.; Rusnak, D.; Shewchuk, L.; Veal, J. M.; Walker, D. H.; Kuyper, L. F. Oxindole-Based Inhibitors of Cyclin-Dependent Kinase 2 (CDK2): Design, Synthesis, Enzymatic Activities, and X-ray Crystallographic Analysis. *J. Med. Chem.* **2001**, *44*, 4339−4358.

(9) Scala, A.; Cordaro, M.; Grassi, G.; Piperno, A.; Barberi, G.; Cascio, A.; Risitano, F. Direct synthesis of C3-mono-functionalized oxindoles from N-unprotected 2-oxindole and their antileishmanial activity. *Bioorg. Med. Chem.* **2014**, *22*, 1063−1069.

(10) For some reviews about spiro-oxindoles, see: (a) Cao, Z.-Y.; Zhou, F.; Zhou, J. Development of Synthetic Methodologies via Catalytic Enantioselective Synthesis of 3,3-Disubstituted Oxindoles. *Acc. Chem. Res.* **2018**, *51*, 1443−1454. (b) Yu, B.; Yu, D.-Q.; Liu, H.-M. Spirooxindoles: Promising scaffolds for anticancer agents. *Eur. J. Med. Chem.* **2015**, *97*, 673−698. (c) Cheng, D.; Ishihara, Y.; Tan, B.; Barbas, C. F., III Organocatalytic Asymmetric Assembly Reactions: Synthesis of Spirooxindoles via Organocascade Strategies. *ACS Catal.* **2014**, *4*, 743−762. (d) Shen, K.; Liu, X.; Lin, L.; Feng, X. Recent Progress in Enantioselective Synthesis of C3-Functionalized Oxindoles: Rare Earth Metals Take Action. *Chem. Sci.* **2012**, *3*, 327−334. (e) Galliford, C. V.; Scheidt, K. A. Pyrrolidinyl-Spirooxindole Natural Products as Inspirations for the Development of Potential Therapeutic Agents. *Angew. Chem., Int. Ed.* **2007**, *46*, 8748−8758.

(11) Zhang, W.; Xu, J.; Cao, J.; Fang, C.; Zhu, J.; Lu, T.; Du, D. N-heterocyclic carbene-mediated formal [3 + 3] annulation of isatin-derived $\alpha$, $\beta$-unsaturated acids: Access to functionalized 3,4′-spirooxindole $\delta$-lactones. *Tetrahedron* **2017**, *73*, 3249−3254.

(12) Hu, H.; Teng, F.; Liu, J.; Hu, W.; Luo, S.; Zhu, Q. Enantioselective Synthesis of 2-Oxindole Spirofused Lactones and Lactams by Heck/Carbonylative Cylization Sequences: Method Development and Applications. *Angew. Chem., Int. Ed.* **2019**, *58*, 9225−9229.

(13) Chung, C. P.; Hsu, C. Y.; Lin, J. H.; Kuo, Y. H.; Chiang, W.; Lin, Y. L. Antiproliferative Lactams and Spiroenone from Adlay Bran in Human Breast Cancer Cell Lines. *J. Agric. Food Chem.* **2011**, *59*, 1185−1194.

(14) Correia, V. G.; Abreu, J. C.; Barata, C. A. E.; Andrade, L. H. Iron-Catalyzed Synthesis of Oxindoles: Application to the Preparation of Pyrroloindolines. *Org. Lett.* **2017**, *19*, 1060−1063.

(15) (a) Yang, D.; Zhang, C. Ruthenium-Catalyzed Oxidative Cleavage of Olefins to Aldehydes. *J. Org. Chem.* **2001**, *66*, 4814−4818. (b) Ojima, I.; Korda, A.; Shay, W. R. New Synthesis of Nitrogen Heterocycles Through Amide-Directed Hydrocarbonylation of Alkenamides Catalyzed by Rhodium Complexes. *J. Org. Chem.* **1991**, *56*, 2024−2030.

(16) Cinquin, C.; Bortolussi, M.; Bloch, R. 2,5-Dihydropyrrole Derivatives as Enantiomerically Enriched Building Blocks: Synthesis of the Geissman-Waiss Lactone and Polyhydroxylated Pyrrolidines. *Tetrahedron: Asymmetry* **1996**, *7*, 3327−3332.



https://dx.doi.org/10.1021/acs.oprd.0c00057
*Org. Process Res. Dev.* XXXX, XXX, XXX−XXX

(17) Winkler, J. D.; Rouse, M. B.; Greaney, M. F.; Harrison, S. J.; Jeon, Y. T. The First Total Synthesis of (±)-Ingenol. *J. Am. Chem. Soc.* **2002**, *124*, 9726−9728.
(18) Ackermann, L.; Lygin, A. V.; Hofmann, N. Ruthenium-Catalyzed Oxidative Synthesis of 2-Pyridones through C−H/N−H Bond Functionalizations. *Org. Lett.* **2011**, *13*, 3278−3281.
(19) Kawasaki, T.; Ogawa, A.; Terashima, R.; Saheki, T.; Ban, N.; Sekiguchi, H.; Sakaguchi, K.; Sakamoto, M. Synthesis of Diversely Functionalized Hexahydropyrrolo[2,3-b]indoles Using Domino Reactions, Olefination, Isomerization and Claisen Rearrangement Followed by Reductive Cyclization. *J. Org. Chem.* **2005**, *70*, 2957−2966.


https://dx.doi.org/10.1021/acs.oprd.0c00057
*Org. Process Res. Dev.* XXXX, XXX, XXX−XXX